An Approach to a Digital Adaptive Controller for guidance of Unmanned Vehicles - Comparison with Digitally-Translated Analog Counterparts

Mario A. Jordán, and Jorge L. Bustamante

Abstract— **This paper deals with the design of a digital adaptive control system for a class of complex dynamics. Though the approach is based on known speed-gradient techniques in continuous time domain, it is directly worked up in the discrete time to ensure the convexity conditions. The approach is compared with analog speed-gradient controllers which are translated directly to the digital time domain. The influence of noisy measures and modelling errors are tracked along with the analysis of stability and performance. A comparative case study concerning the guidance of unmanned vehicles for path tracking illustrates the features of the approaches in this application field.\end{abstract**

Keywords— **Digital adaptive control systems, Nonlinear dynamics, noisy measures, modelling errors, stability, unmanned vehicles, path tracking.**

I. Introduction

Tools and systematic procedures to design adaptive control systems have been developed extensively in the past decade oriented to general classes of nonlinear systems with uncertainties. The methods however are dominantly represented by designs in continuous time [Krstić *et al.*, 1995], [Fradkov *et al.*, 1999].

When applying digital technology, both in computing and communication, the implementation of controllers in digital form is unavoidable. Additionally, in many applications, the sensorial components work inherently digitally as samplers [Kinsey *et al.*, 2006]. This is the case of unmanned vehicles, which will be the application framework here.

The translation of extended analog-controller design approaches for underwater vehicles to the discrete-time domain is commonly done by a simple digitalization of the controlling action, and in the case of adaptive controllers, of the adaptive laws too [Antonelli, 2006], [Smallwood and Whitcomb, 2003].

This way generally provides a good control system behavior, however the role played by the sampling time in the stability and performance must be cautiously investigated due to potential instability.

Additionally noisy measures and digitalization errors may not only affect the stability properties significantly but also increase the complexity of the analysis.

Corresponding Author: Mario A. Jordán: E-mail: mjordan@criba.edu.ar. Address: CCT-CONICET. Florida 8000, B8000FWB, Bahía Blanca, ARGENTINA

Mario Jordán and Jorge Bustamante are with the Argentine Institute of Oceanography (IADO-CONICET) and Dto. de Ingeniería Eléctrica y de Computadoras (DIEC-UNS), Bahía Blanca, Argentina.

In this paper we attempt to research the path tracking sampled-data control with two alternatives. One way is the usual translation of a designed analog controller to the digital domain. The second way is the direct design in the discrete-time domain upon approximative models. Both ways rest on the same design procedure. This last design is the original contribution of the paper, while the comparison with the most-extended design technique describes the way by which we valorize the features of our approach.

II. Particular dynamics class

Many systems are described as the conjugation of two ODEs in generalized variables, namely one for the kinematics and the other one for the inertia (see Fig. 1). The block structure embraces a wide range of vehicle systems like mobile robots, unmanned aerial vehicles, spacecraft and satellite systems, autonomous underwater vehicles (AUV) or remotely operated vehicles (ROV), though with slight distinctive modifications in the structure among them.

The vehicle dynamics is widely described in the literature [*cf.* Fossen, 1994]

$$\dot{\mathbf{v}}=M^{-1}\left(-C(\mathbf{v})\mathbf{v}-D(|\mathbf{v}|)\mathbf{v}+\mathbf{g}(\boldsymbol{\eta})+\boldsymbol{\tau}_c+\boldsymbol{\tau}\right) \quad (1)$$

$$\dot{\boldsymbol{\eta}}=J(\boldsymbol{\eta})(\mathbf{v}+\mathbf{v}_c). \quad (2)$$

Here $\boldsymbol{\eta}=[x,y,z,\varphi,\theta,\psi]^T$ is the generalized position vector and components referred on a earth-fixed frame, and $\mathbf{v}=[u,v,w,p,q,r]^T$ is the generalized rate vector referred on a vehicle-fixed frame. Other variables of the dynamics and control system are indicated in the Fig. 1 self.

The matrices M, C and D are the inertia, the Coriolis-centripetal and the drag matrices, respectively, $\mathbf{g}$ is the buoyancy vector and J is the rotation matrix expressing the transformation from the inertial frame to the vehicle-fixed frame.

For future developments in the controller design, it is valid [Jordán and Bustamante, 2009]

$$M = M_a + M_b \quad (3)$$

$$C(\mathbf{v}) = \sum_{i=1}^{6} C_i. \times C_{v_i}(v_i) \quad (4)$$

$$D(|\mathbf{v}|) = D_l + \sum_{i=1}^{6} D_{q_i}\ |v_i| \quad (5)$$

$$\mathbf{g}(\boldsymbol{\eta}) = -B_1\ \mathbf{g}_1(\boldsymbol{\eta}) - B_2\mathbf{g}_2(\boldsymbol{\eta}) \tag{6}$$

where M_b the body inertia and M_a the additive mass. The matrices C_i, D_l, D_{q_i}, B_1 and B_2 are constant and supposed unknown, while $C_{v_i}, \mathbf{g}_1$ and $\mathbf{g}_2$ are state-dependent and computable arrays and v_i is an element of $\mathbf{v}$. Finally ".×" is an element-by-element array product.

A. Sampled-data behavior

For the continuous-time dynamics there exists an associated exact sampled-data dynamics described by the set of sequences $\{\boldsymbol{\eta}(t_i), \mathbf{v}(t_i)\} = \{\boldsymbol{\eta}_{t_i}, \mathbf{v}_{t_i}\}$ with a sampling rate h.

In the presence of measure disturbances $\delta\boldsymbol{\eta}_{t_n}$ and $\delta\mathbf{v}_{t_n}$, the samples are represented by $\{\boldsymbol{\eta}_\delta(t_i), \mathbf{v}_\delta(t_i)\} = \{\boldsymbol{\eta}_{\delta_{t_i}}, \mathbf{v}_{\delta_{t_i}}\}$ (see Fig. 1). Moreover, we will concentrate on the influence of measure disturbances and of model errors on the stability when no exogenous perturbations are present. In this way we have $\boldsymbol{\tau}_c = \mathbf{v}_c = 0$, $\mathbf{v} = \bar{\mathbf{v}}$ and $\boldsymbol{\eta} = \bar{\boldsymbol{\eta}}$. For details of the influence of perturbations and model errors in the control, the reader can referred to a study in [Jordán and Bustamante, 2008] and [Jordán and Bustamante, 2007], respectively.

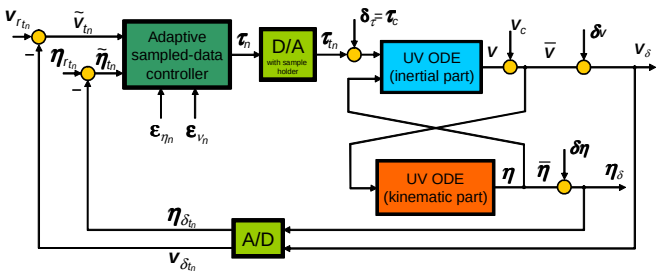

Fig. 1 - Digital adaptive control system for underwater vehicles

B. Sampled-data model

Let (1)-(2) be described in a compact form by

$$\dot{\mathbf{v}} = M^{-1}\mathbf{p}(\boldsymbol{\eta},\mathbf{v}) + M^{-1}\boldsymbol{\tau} \tag{7}$$
$$\dot{\boldsymbol{\eta}} = \mathbf{q}(\boldsymbol{\eta},\mathbf{v}), \tag{8}$$

with $\mathbf{p}$ and $\mathbf{q}$ being Lipschitz vector functions located at the right-hand memberships. Now, employing a one-step-ahead predictor (see [Jordán *et al.*, 2010] for higher order Adams-Bashforth approximators)

$$\mathbf{v}_{n+1} = \mathbf{v}_{t_n} + h\left(M^{-1}\mathbf{p}_{t_n} + M^{-1}\boldsymbol{\tau}_n\right) \tag{9}$$
$$\boldsymbol{\eta}_{n+1} = \boldsymbol{\eta}_{t_n} + h\mathbf{q}_{t_n}, \tag{10}$$

where $\boldsymbol{\eta}_{n+1}$ and $\mathbf{v}_{n+1}$ are one-step-ahead predictions at the present time step t_n. Moreover, $\boldsymbol{\tau}_n$ is the discrete-time control action at t_n, which is equal to the sample $\boldsymbol{\tau}(t_n)$ because of the employed zero-order sample holder.

More precisely it is valid with (1)-(2)

$$\mathbf{p}_{t_n} = -\left(\sum_{i=1}^{6} C_i. \times C_{v_{i_{t_n}}}\mathbf{v}_{t_n} + D_l\mathbf{v}_{t_n} + \right. \tag{11}$$
$$\left. + \sum_{i=1}^{6} D_{q_i}\ |v_{i_{t_n}}|\mathbf{v}_{t_n} + B_1\ \mathbf{g}_{1_{t_n}} + B_2\ \mathbf{g}_{2_{t_n}}\right)$$
$$\mathbf{q}_{t_n} = J_{t_n}\mathbf{v}_{t_n} \tag{12}$$

where $\mathbf{v}_{t_n}$ marks the dependence of a variable with the sampling time.

We define local model errors as

$$\boldsymbol{\varepsilon}_{v_{n+1}} = \mathbf{v}_{t_{n+1}} - \mathbf{v}_{n+1} \tag{13}$$
$$\boldsymbol{\varepsilon}_{\eta_{n+1}} = \boldsymbol{\eta}_{t_{n+1}} - \boldsymbol{\eta}_{n+1}, \tag{14}$$

with $\boldsymbol{\varepsilon}_{\eta_{n+1}}$, $\boldsymbol{\varepsilon}_{v_{n+1}} \in \mathcal{O}(h)$ and $\mathcal{O}$ an order of magnitude function.

Since $\mathbf{p}$ and $\mathbf{q}$ are Lipschitz continuous, the samples, predictions and local errors all yield bounded. So it is valid the property $\mathbf{v}_{n+1} \to \mathbf{v}_{t_{n+1}}$ and $\boldsymbol{\eta}_{n+1} \to \boldsymbol{\eta}_{t_{n+1}}$ for $h \to 0$.

C. 1st-order predictor with disturbances

By the presence of disturbances it is valid from (9)-(10)

$$\mathbf{v}_{n+1} = \mathbf{v}_{t_n} + \delta\mathbf{v}_{t_n} + hM^{-1}\mathbf{p}\left(\mathbf{v}_{t_n} + \boldsymbol{\delta}\mathbf{v}_{t_n}, \boldsymbol{\eta}_{t_n} + \delta\boldsymbol{\eta}_{t_n}\right) + \tag{15}$$
$$+ hM^{-1}\boldsymbol{\tau}_n$$
$$\boldsymbol{\eta}_{n+1} = \boldsymbol{\eta}_{t_n} + \delta\boldsymbol{\eta}_{t_n} + h\mathbf{q}\left(\mathbf{v}_{t_n} + \boldsymbol{\delta}\mathbf{v}_{t_n}, \boldsymbol{\eta}_{t_n} + \delta\boldsymbol{\eta}_{t_n}\right), \tag{16}$$

where $\delta\mathbf{v}_{t_n}$ and $\delta\boldsymbol{\eta}_{t_n}$ are the measure disturbances (*cf.* Fig. 1) and $\mathbf{p}_{\delta_{t_n}}$ and $\mathbf{q}_{\delta_{t_n}}$ are perturbed functions $\mathbf{p}$ and $\mathbf{q}$, respectively.

III. Design I: Sampled-data adaptive controller

The first goal in the paper is to design a general class of adaptive control systems in a discrete time domain directly. The control problem is focused to the path tracking of a geometric reference $\boldsymbol{\eta}_{r_{t_n}}$ as well as of a kinematic reference $\mathbf{v}_{r_{t_n}}$ (*cf.* Fig. 1).

For the following cost function

$$Q_{t_n} = \overset{\frown}{\boldsymbol{\eta}}{}^T_{t_n}\overset{\frown}{\boldsymbol{\eta}}_{t_n} + \overset{\frown}{\mathbf{v}}{}^T_{t_n}\overset{\frown}{\mathbf{v}}_{t_n}. \tag{17}$$

the ideal situation demands that

$$\lim_{t_n \to \infty} Q_{t_n} = 0, \tag{18}$$

A. Control action

Let us try out first the following change of coordinates

$$\overset{\frown}{\boldsymbol{\eta}}_{t_n} = \boldsymbol{\eta}_{t_n} + \delta\boldsymbol{\eta}_{t_n} - \boldsymbol{\eta}_{r_{t_n}} \tag{19}$$
$$\overset{\frown}{\mathbf{v}}_{t_n} = \mathbf{v}_{t_n} + \delta\mathbf{v}_{t_n} - J^{-1}_{\delta_{t_n}}\dot{\boldsymbol{\eta}}_{r_{t_n}} + J^{-1}_{\delta_{t_n}}K_p\overset{\frown}{\boldsymbol{\eta}}_{t_n}. \tag{20}$$

where $K_p = K_p^T \geq 0$ is a design gain matrix affecting the geometric path errors and the subscript "$_{\delta_{t_n}}$" means a variable that is perturbed with noisy measures. Clearly, if $\overset{\frown}{\boldsymbol{\eta}}_{t_n} \equiv \mathbf{0}$, then by (20) and (2), it yields $\mathbf{v}_{t_n} + \delta\mathbf{v}_{t_n} - \mathbf{v}_{r_{t_n}} \equiv \mathbf{0}$, with $\mathbf{v}_{t_n}$ close to $\mathbf{v}_{r_{t_n}}$ with error $\delta\mathbf{v}_{t_n}$ as in Fig. 1.

Employing (15) and (16) in (19) and in (20), and finally the last both equation in (17), one obtains after some calculations

$$\Delta Q_{t_n} = Q_{t_{n+1}} - Q_{t_n} = \Big((I - hK_p)\,\overset{\frown}{\boldsymbol{\eta}}_{t_n} + h\left(J_{\delta_{t_n}} \overset{\frown}{\mathbf{v}}_{t_n} + \dot{\boldsymbol{\eta}}_{r_{t_n}} \right) + \\ + \boldsymbol{\eta}_{r_{t_n}} - \boldsymbol{\eta}_{r_{t_{n+1}}} + \boldsymbol{\varepsilon}_{\eta_{n+1}} + \delta\boldsymbol{\eta}_{t_{n+1}} \Big)^2 - \overset{\frown}{\boldsymbol{\eta}}_{t_n}^2 + \\ + \Big(\overset{\frown}{\mathbf{v}}_{t_n} + J_{\delta_{t_n}}^{-1} \dot{\boldsymbol{\eta}}_{r_{t_n}} - J_{\delta_{t_n}}^{-1} K_p \overset{\frown}{\boldsymbol{\eta}}_{t_n} - J_{\delta_{t_{n+1}}}^{-1} \dot{\boldsymbol{\eta}}_{r_{t_{n+1}}} + J_{\delta_{t_{n+1}}}^{-1} K_p \overset{\frown}{\boldsymbol{\eta}}_{t_{n+1}} + \\ + h\Big(M^{-1} \mathbf{p}_{\delta_{t_n}} + M^{-1} \boldsymbol{\tau}_n \Big) + \delta\mathbf{v}_{t_{n+1}} + \boldsymbol{\varepsilon}_{v_{n+1}} \Big)^2 - \overset{\frown}{\mathbf{v}}_{t_n}^2. \quad (21)$$

We can now conveniently split the control thrust $\boldsymbol{\tau}_n$ into two terms as

$$\boldsymbol{\tau}_n = \boldsymbol{\tau}_{1_n} + \boldsymbol{\tau}_{2_n}, \quad (22)$$

The first term, $\boldsymbol{\tau}_{1_n}$, serves to neutralize some specific terms in (21) with nondefinite sign. Thus

$$\boldsymbol{\tau}_{1_n} = -K_v \overset{\frown}{\mathbf{v}}_{t_n} - \frac{1}{h} \underline{M} \Big(J_{\delta_{t_n}}^{-1} \dot{\boldsymbol{\eta}}_{r_{t_n}} + J_{\delta_{t_n}}^{-1} K_p \overset{\frown}{\boldsymbol{\eta}}_{t_n} + \\ + J_{\delta_{t_{n+1}}}^{-1} \dot{\boldsymbol{\eta}}_{r_{t_{n+1}}} - J_{\delta_{t_{n+1}}}^{-1} K_p \overset{\frown}{\boldsymbol{\eta}}_{t_{n+1}} \Big) - \mathbf{r}_{\delta_{t_n}}, \quad (23)$$

with $K_v = K_v^T \geq 0$ another design gain matrix for affecting the kinematic errors, and $\mathbf{r}_{\delta_{t_n}}$ being

$$\mathbf{r}_{\delta_{t_n}} = -\sum_{i=1}^{6} U_{i_n} . \times C_{v_{i_{t_n}}} \mathbf{v}_{\delta_{t_n}} - U_{7_n} \mathbf{v}_{\delta_{t_n}} - \\ - \sum_{i=1}^{6} U_{7+i_n} |v_{i_{t_n}}| \mathbf{v}_{\delta_{t_n}} + U_{14_n} \mathbf{g}_{1_{\delta_{t_n}}} + U_{15_n}\, \mathbf{g}_{2_{\delta_{t_n}}}, \quad (24)$$

where the matrices U_i will account for every unknown system matrix in the partial control action $\boldsymbol{\tau}_{1_n}$ with the unique exception of the inertia matrix M from which only a lower bound $\underline{M}$ is demanded. The construction of the U_i´s is defined later as part of the design of the adaptive controller.

Putting $\boldsymbol{\tau}_{1_n}$ in ΔQ_{t_n}, it only remains the definition of $\boldsymbol{\tau}_{2_n}$. Certainly, with $K_v^* \triangleq M^{-1} K_v$ one gets

$$\Delta Q_{t_n} = h^2 (M^{-1} \boldsymbol{\tau}_{2_n})^2 + \mathbf{b}_n^T M^{-1} \boldsymbol{\tau}_{2_n} + c_n + \\ + \overset{\frown}{\boldsymbol{\eta}}_{t_n}^T hK_p \,(hK_p - 2I)\, \overset{\frown}{\boldsymbol{\eta}}_{t_n} + \overset{\frown}{\mathbf{v}}_{t_n}^T hK_v^* \Big(hK_v^* - 2I \Big) \overset{\frown}{\mathbf{v}}_{t_n} + \\ + f_{U_i}((U_i^* - U_i)\,, \Big(I - M^{-1} \underline{M} \Big)) + \\ + f_{\varepsilon,\delta}(\boldsymbol{\varepsilon}_{\eta_{n+1}}, \boldsymbol{\varepsilon}_{v_{n+1}}, \delta\boldsymbol{\eta}_{t_{n+1}}, \delta\mathbf{v}_{t_{n+1}})\,, \quad (25)$$

where $\mathbf{b}_n$ and c_n are variables of the geometric and kinematic path errors and the respective path references, model errors and disturbances, and finally of the controller and system matrices. The functions f_{U_i} and $f_{\varepsilon,\delta}$ are sign-nondefined scalar functions. They both satisfy

$$\lim_{U_i \to U_i^*} f_{U_i} = 0 \quad \text{and} \quad \lim_{\varepsilon,\delta \to 0} f_{\varepsilon,\delta} = 0, \quad (26)$$

where the U_i's are the controller matrices and the U_i^*'s are the system matrices assigned as

$$U_i^* = C_i, \text{ with } i = 1, ...6 \quad (27)$$

$$U_7^* = D_l\,, \qquad U_i^* = D_{q_i}, \text{ with } i = 8, ...13 \quad (28)$$

$$U_{14}^* = B_1 \qquad \text{and} \qquad U_{15}^* = B_2\,. \quad (29)$$

For space limitations in the paper we do not transcribe analytical expressions for $\mathbf{b_n}$, c_n, f_{U_i} and $f_{\varepsilon,\delta}$, which are obtained after some calculations by inserting (11), (23), (22) and (24) in (21).

Now, the functional can be minimized by choosing the second component of the control action, it is $\boldsymbol{\tau}_{2_n}$, properly. For instance

$$h^2 \left(M^{-1} \boldsymbol{\tau}_{2_n} \right)^2 + \overline{\mathbf{b}}_n^T M^{-1} \boldsymbol{\tau}_{2_n} + \bar{c}_n = 0. \quad (30)$$

where $\overline{\mathbf{b}}_n$ and $\bar{c}_n$ are variables of the measured geometric and kinematic path errors and their respective path references only. Unlike $\mathbf{b}_n$ and c_n in (21), $\overline{\mathbf{b}}_n$ and $\bar{c}_n$ are implementable.

So, to fulfill (30), we choose

$$\boldsymbol{\tau}_{2_n} = \underline{M}\ \overline{\boldsymbol{\tau}}_{2_n}, \quad (31)$$

with

$$\overline{\boldsymbol{\tau}}_{2_n} = \frac{-\overline{\mathbf{b}}_n}{2h^2} \pm \frac{1}{2h^2} \sqrt{\frac{\overline{\mathbf{b}}_n^T \overline{\mathbf{b}}_n - 4h^2\, \bar{c}_n}{6}}\, \mathbf{o}. \quad (32)$$

In order to implement $\boldsymbol{\tau}_{2_n}$ while eventually there does not exist real roots in (32), one can chose the real part of the resulting complex roots, namely $\overline{\boldsymbol{\tau}}_{2_n} = \frac{-\overline{\mathbf{b}}_n}{2h^2}$. The implications of this choice in the stability of the control system will be analyzed later.

So the control action to be applied to the vehicle system is $\boldsymbol{\tau}_n = \boldsymbol{\tau}_{1_n} + \boldsymbol{\tau}_{2_n}$ with the two components given in (23) and (31), respectively.

B. Ideal adaptive laws

According to the speed-gradient law suggested by [Fradkov *et al.*, 1999], the adaptation of the system behavior occurs with the permanent actualization of the controller matrices U_i´s

$$U_{i_{n+1}} \triangleq U_{i_n} - \Gamma_i \frac{\partial \Delta Q_{t_n}}{\partial U_i}, \quad (33)$$

with a gain matrix $\Gamma_i = \Gamma_i^T \geq 0$ and $\frac{\partial \Delta Q_{t_n}}{\partial U_{i_n}}$ being a gradient matrix for U_{i_n}.

For convenience we first define an expression for the gradient matrix upon ΔQ_{t_n} in (25) with the consideration that M is known. This expression is referred to the ideal gradient matrix

$$\frac{\partial \Delta Q_{t_n}}{\partial U_i} = -2h^2 M^{-T} \left(M^{-1} \boldsymbol{\tau}_{2_n} \right) \left(\frac{\partial \mathbf{r}_{\delta_{t_n}}}{\partial U_i} \right)^T - \\ -2h^2 M^{-T} M^{-1} (\mathbf{p}_{\delta_{t_n}} - \mathbf{r}_{\delta_{t_n}}) \left(\frac{\partial \mathbf{r}_{\delta_{t_n}}}{\partial U_i} \right)^T - \\ -2hM^{-T} (I - hK_v^*) \overset{\frown}{\mathbf{v}}_{t_n} \left(\frac{\partial \mathbf{r}_{\delta_{t_n}}}{\partial U_i} \right)^T. \quad (34)$$

Next we derive a real counterpart of $\frac{\partial \Delta Q_{t_n}}{\partial U_i}$.

C. Practical adaptive laws

The unknown M in (34) is replaced by its lower bound $\underline{M}$. Moreover, the term $\mathbf{p}_{\delta_{t_n}}$ is unknown and can not be reconstructed exactly from $\mathbf{p}_{\delta_{t_n}} = \mathbf{M}\dot{\mathbf{v}}_{t_n} - \boldsymbol{\tau}_n =$, instead we replace it by $\overline{\mathbf{p}}_{\delta_{t_n}} = \underline{M}\frac{\mathbf{v}_{t_n} - \mathbf{v}_{t_{n-1}}}{h} - \boldsymbol{\tau}_n$.

In this way, we can generate implementable gradient matrices which will denote by $\frac{\partial \overline{\Delta Q}_{t_n}}{\partial U_i}$. So following relations can be established for $i \geq 1$

$$\frac{\partial \overline{\Delta Q}_{t_n}}{\partial U_i} = \frac{\partial \Delta Q_{t_n}}{\partial U_i} + \Delta_{U_{i_n}}, \tag{35}$$

with

$$\Delta_{U_{i_n}} = \delta_{M^{-2}} A_{i_n} + \delta_{M^{-1}} B_{i_n}, \tag{36}$$

where $\delta_{M^{-2}} = \left(\underline{M}^{-T}\underline{M}^{-1} - M^{-T}M^{-1}\right) \geq 0$ and $\delta_{M^{-1}} = \left(\underline{M}^{-1} - M^{-1}\right) \geq 0$. Here A_{i_n} and B_{i_n} are sampled state functions obtained from (34) after extracting of the common factors $\delta_{M^{-2}}$ and $\delta_{M^{-1}}$, respectively.

It is worth noticing that ΔQ_{t_n} and $\overline{\Delta Q}_{t_n}$ (it is, ΔQ_{t_n} with $\underline{M}^{-1}$ instead of M^{-1}), satisfy convexity properties in the space of elements of the U_i's. Moreover, with (35) in mind we can conclude for any pair of values of U_{i_n}, say U'_{i_n} of U''_{i_n}, it is valid

$$\Delta Q_{t_n}(U'_{i_n}) - \Delta Q_{t_n}(U''_{i_n}) \leq \frac{\partial \Delta Q_{t_n}(U''_{i_n})}{\partial U_i}\left(U'_{i_n} - U''_{i_n}\right) \leq \tag{37}$$

$$\leq \frac{\partial \overline{\Delta Q}_{t_n}(U''_{i_n})}{\partial U_i}\left(U'_{i_n} - U''_{i_n}\right). \tag{38}$$

This feature will be useful in the next analysis.

D. Stability analysis

First let $\Delta Q^*_{t_n}$ be the same functional as (25) but with $\boldsymbol{\tau}_{2_n}$ and $U^*_i = U_i$ in (27)-(29), so $f_{U_i} = 0$ and

$$\Delta Q^*_{t_n} = \widehat{\boldsymbol{\eta}}^{T}_{t_n} h K_p (hK_p - 2I)\,\widehat{\boldsymbol{\eta}}_{t_n} + \widehat{\mathbf{v}}^{T}_{t_n} h K_v (hK^*_v - 2I)\,\widehat{\mathbf{v}}_{t_n} + \tag{39}$$

$$+ f^*_{\Delta Q_n}[\boldsymbol{\varepsilon}_{\eta_{n+1}}, \boldsymbol{\varepsilon}_{v_{n+1}}, \delta\boldsymbol{\eta}_{t_n}, \delta\mathbf{v}_{t_n}, M^{-1}\underline{M}],$$

with

$$f^*_{\Delta Q_n} = f_{U_i}(U^*_i = U_i, \left(I - M^{-1}\underline{M}\right)) + \tag{40}$$

$$+ f_{\varepsilon,\delta}(\boldsymbol{\varepsilon}_{\eta_{n+1}}, \boldsymbol{\varepsilon}_{v_{n+1}}, \delta\boldsymbol{\eta}_{t_{n+1}}, \delta\mathbf{v}_{t_{n+1}}).$$

Since $\left(\boldsymbol{\varepsilon}_{v_{n+1}} + \delta\mathbf{v}_{t_{n+1}}\right), \left(\boldsymbol{\varepsilon}_{v_{n+1}} + \delta\mathbf{v}_{t_{n+1}}\right)$ and $M^{-1}\underline{M} \in l_\infty$, then one can conclude that $f^*_{\Delta Q_n} \in l_\infty$ as well (this can be accomplished by putting $\boldsymbol{\tau}_n = \boldsymbol{\tau}_{1n} + \boldsymbol{\tau}_{2_n}$ in (21) and isolating the terms with the perturbations).

It is noticing that the quadratic form fulfills $\Delta Q^*_{t_n} < 0$, at least in an attraction domain equal to $\mathcal{B} = \left\{\widehat{\boldsymbol{\eta}}_{t_n}, \widehat{\mathbf{v}}_{t_n} \in \mathcal{R}^6 \cap \mathcal{B}^*_{0_n}\right\}$ with $\mathcal{B}^*_{0_n}$ a residual set around zero with

$$\mathcal{B}^*_{0_n} = \left\{\widehat{\boldsymbol{\eta}}_{t_n}, \widehat{\mathbf{v}}_{t_n} \in \mathcal{R}^6 / \Delta Q^*_{t_n} - f^*_{\Delta Q_n} \leq 0\right\} \tag{41}$$

and with the design matrices satisfying the conditions

$$\frac{2}{h}I > K_p \geq 0 \quad \text{and} \quad \frac{2}{h}I > K^*_v \geq 0, \tag{42}$$

with $K^*_v = M^{-1}K_v$, which is equivalent to

$$\frac{2}{h}M \geq \frac{2}{h}\underline{M} > K_v \geq 0. \tag{43}$$

The residual set $\mathcal{B}^*_0$ depends not only on $\boldsymbol{\varepsilon}_{\eta_{n+1}}$ and $\boldsymbol{\varepsilon}_{v_{n+1}}$ and the measure noises $\delta\boldsymbol{\eta}_{t_n}$ and $\delta\mathbf{v}_{t_n}$, but also on $M^{-1}\underline{M}$. In consequence, $\mathcal{B}^*_0$ becomes the null point at the limit when $h \to 0$, $\delta\boldsymbol{\eta}_{t_n}$, $\delta\mathbf{v}_{t_n} \to 0$ and $\underline{M} = M$.

Next, for proving stability of the adaptive control system let a candidate Lyapunov function be

$$V_{t_n} = Q_{t_n} + \frac{1}{2}\sum_{i=1}^{15}\sum_{j=1}^{6}\left(\widetilde{\mathbf{u}}^T_j\right)_{i_{n+1}} \Gamma_i^{-1}\left(\widetilde{\mathbf{u}}_j\right)_{i_{n+1}} - \tag{44}$$

$$-\frac{1}{2}\sum_{i=1}^{15}\sum_{j=1}^{6}\left(\widetilde{\mathbf{u}}^T_j\right)_{i_n} \Gamma_i^{-1}\left(\widetilde{\mathbf{u}}_j\right)_{i_n},$$

with $\left(\widetilde{\mathbf{u}}_j\right)_{i_n} = \left(\mathbf{u}_j - \mathbf{u}^*_j\right)_{i_n}$, where $\mathbf{u}_j$ and $\mathbf{u}^*_j$ are vectors corresponding to the column j of the adaptive controller matrix U_{i_n} and its homologous one U^*_i, respectively. Then, taking $\Delta V_{t_n} = V_{t_{n+1}} - V_{t_n}$ it is valid

$$\Delta V_{t_n} = \Delta Q_{t_n} + \sum_{i=1}^{15}\sum_{j=1}^{6}\left(\Delta\mathbf{u}^T_j\right)_{i_n} \Gamma_i^{-1}\left(\widetilde{\mathbf{u}}_j\right)_{i_n} - \tag{45}$$

$$-\frac{1}{2}\sum_{i=1}^{15}\sum_{j=1}^{6}\left(\Delta\mathbf{u}^T_j\right)_{i_n} \Gamma_i^{-1}\left(\Delta\mathbf{u}_j\right)_{i_n} \leq$$

$$\leq \Delta Q_{t_n} - \sum_{i=1}^{15}\sum_{j=1}^{6}\left(\frac{\partial \Delta Q_{t_n}}{\partial \mathbf{u}_j}\right)^T\left(\widetilde{\mathbf{u}}_j\right)_{i_n} \leq$$

$$\leq \Delta Q_{t_n} - \sum_{i=1}^{15}\sum_{j=1}^{6}\left(\frac{\partial \overline{\Delta Q}_{t_n}}{\partial \mathbf{u}_j}\right)^T\left(\widetilde{\mathbf{u}}_j\right)_{i_n} \leq \Delta Q^*_{t_n} < 0 \text{ in } \mathcal{B} \cap \mathcal{B}^*_0,$$

with $\left(\Delta\mathbf{u}_j\right)_{i_n}$ a column vector of $\left(U_{i_{n+1}} - U_{i_n}\right)$. At the first inequality, the adaptive law (33) for the column vector $\left(\Delta\mathbf{u}_j\right)_{i_n}$ was replaced by the column vector $-\Gamma_i\left(\frac{\partial \Delta Q_{t_n}}{\partial \mathbf{u}_j}\right)$ and then by $-\Gamma_i\left(\frac{\partial \overline{\Delta Q}_{t_n}}{\partial \mathbf{u}_j}\right)$ in the right member according to (35) and (37)-(38). So in the second and third inequality, the convexity property of ΔQ_{t_n} in (37) was applied for any pair $(U' = U_{i_n}, U'' = U^*_i)$.

This analysis has proved convergence of the error paths when real roots exist in the equation $\sqrt{\overline{\mathbf{b}}^T_n\overline{\mathbf{b}}_n - 4\,\bar{a}\,\bar{c}_n}$ of (31).

If on the contrary $4h^2\bar{c}_n > \overline{\mathbf{b}}^T_n\overline{\mathbf{b}}_n$ occurs at some time t_n, one chooses the real part of the complex roots in (31). So a suboptimal control action is employed instead equal to

$$\boldsymbol{\tau}_{2_n} = \frac{-1}{2h^2}\underline{M}\overline{\mathbf{b}}_n = \frac{-\underline{M}}{h}(I - hK^*_v)\widehat{\mathbf{v}}_{t_n}, \tag{46}$$

and yields a new functional $\Delta Q^{**}_{t_n}$ in

$$\Delta V_{t_n} \leq \Delta Q^{**}_{t_n} = \Delta Q^{*}_{t_n} + \bar{c}_n - \frac{1}{4h^2}\overline{\mathbf{b}}_n^{T}\overline{\mathbf{b}}_n < 0 \text{ in } \mathcal{B}\cap\mathcal{B}^{**}_0, \tag{47}$$

where $\Delta Q^{*}_{t_n}$ is (39) with a real root of (31) and $\mathcal{B}^{**}_0$ is a new residual set. It is worth noticing that the positive quantity $\left(\bar{c}_n - \frac{1}{4h^2}\overline{\mathbf{b}}_n^{T}\overline{\mathbf{b}}_n\right)$ can be reduced by choosing h small. Nevertheless, $\mathcal{B}^{**}_0$ results larger than $\mathcal{B}^{*}_0$ in (45), since its magnitude depends not only on $\boldsymbol{\varepsilon}_{\eta_{n+1}}$ and $\boldsymbol{\varepsilon}_{v_{n+1}}$ but also on the magnitude of $\left(\bar{c}_n - \frac{1}{4h^2}\overline{\mathbf{b}}_n^{T}\overline{\mathbf{b}}_n\right)$.

E. Summary of the adaptive control algorithm I

The adaptive control algorithm I can be summarized as follows.

Preliminaries:

1) Estimate a lower bound $\underline{M}$, for instance $\underline{M} = M_b$,

2) Define design gain matrices K_p and K_v according to (42)-(43),

3) Define the adaptive gain matrices Γ_i (usually $\Gamma_i = \alpha_i I$ with $\alpha_i > 0$),

4) Define the desired sampled-data path references for the geometric and kinematic trajectories in 6 DOFs: $\boldsymbol{\eta}_{r_{t_n}}$ and $\mathbf{v}_{r_{t_n}}$, respectively.

Continuously at each sample point:

5) Calculate the control thrust $\boldsymbol{\tau}_n$ with components $\boldsymbol{\tau}_{1_n}$in (23) and $\boldsymbol{\tau}_{2_n}$ (31) (or (46)), respectively,

6) Calculate the adaptive controller matrices (34) with the lower bound $\underline{M}$ instead of M.

Long-term tuning:

7) Redefine K_p and K_v in order to achieve optimal tracking performance.

IV. Design II: Digitalized analog adaptive controller

A homologous adaptive speed-gradient-based method in the analog form was published in [Jordán and Bustamante, 2008]. The design leads however to analog adaptive laws that looks more simple instead that the digital counterpart of design I. So we will attempt to describe and employ the digitalized analog laws to the same dynamics (1)-(6) of Section 2.

Thus we depart from the analog control feedback law

$$\boldsymbol{\tau}=\sum_{i=1}^{6} U_i . \times C_{v_i}(v_i)\mathbf{v}+U_{\gamma}\mathbf{v}+\sum_{i=1}^{6} U_{i+\gamma}\,|v_i|\,\mathbf{v}+ \tag{48}$$

$$+U_{14}\mathbf{g}_1+U_{15}\mathbf{g}_2+U_{16}\mathbf{d}-K_v\tilde{\mathbf{v}}-J^{T}\tilde{\boldsymbol{\eta}}\,,$$

with

$$\mathbf{d}=\frac{d}{dt}\left(J^{-1}(\boldsymbol{\eta})\dot{\boldsymbol{\eta}}_r\right)-\frac{dJ^{-1}(\boldsymbol{\eta})}{dt}K_p\tilde{\boldsymbol{\eta}}+ \tag{49}$$

$$+J^{-1}(\boldsymbol{\eta})K_p^{2}\tilde{\boldsymbol{\eta}}-J^{-1}(\boldsymbol{\eta})K_pJ(\boldsymbol{\eta})\tilde{\mathbf{v}}\,.$$

where K_p and K_v are design matrices with similar meaning as in the previous design. The U_i's are the matrices of the adaptive controller obtained by speed-gradient laws [Fradkov *et al.*, 1999]

$$\dot{U}_i = -\Gamma_i\frac{\partial\dot{Q}(U_i)}{\partial U_i}, \tag{50}$$

where $\Gamma_i = \Gamma_i^{T} \geq 0$ are design matrices for the adaptive laws. Herein $Q = \frac{1}{2}\tilde{\boldsymbol{\eta}}^{T}\tilde{\boldsymbol{\eta}} + \frac{1}{2}\tilde{\mathbf{v}}^{T}M\tilde{\mathbf{v}}$ is the proposed functional from which the analog control action (48) was built up.

In order to obtain a digital counterpart of (48), we can at this point simply digitalize $\boldsymbol{\tau}$ to obtain a discrete-time sequence $\boldsymbol{\tau}_n$ as function of samples of the states, namely $\boldsymbol{\eta}_{t_n}$ and $\mathbf{v}_{t_n}$, of the references, namely $\boldsymbol{\eta}_{r_{t_n}}$ and $\mathbf{v}_{r_{t_n}}$.

At this point, it is convenient to construct the sequence $\mathbf{d}_{t_n}$ for $\boldsymbol{\tau}_n$ in (48) not as simple samples from (49), but also by using incremental quotient on the derivatives $\frac{dJ^{-1}(\boldsymbol{\eta})}{dt}$. So, one achieves

$$\mathbf{d}_{t_n}=h^{-1}\Big(J_{t_n}^{-1}\Big(\dot{\boldsymbol{\eta}}_{r_{t_n}}-K_p\tilde{\boldsymbol{\eta}}_{t_n}\Big)-J_{t_{n+1}}^{-1}\Big(\dot{\boldsymbol{\eta}}_{r_{t_{n+1}}}-K_p\tilde{\boldsymbol{\eta}}_{t_{n+1}}\Big)\Big). \tag{51}$$

Finally the actualizations of U_{i_n} are calculated as

$$U_{i_{n+1}} = U_{i_n} - h\Gamma_i\left.\frac{\partial\dot{Q}(U_i)}{\partial U_i}\right|_{t_n}. \tag{52}$$

for $n = 0, 1, 2, ...$

Summarizing, (48), (51) and (52) will be the basic equations of the new digital design.

A. Stability analysis

To this end we can as usually calculate increments $\Delta Q_{t_n} = Q_{t_{n+1}} - Q_{t_n}$ from Q so as to prove stability of the discretized adaptive control system with feedback sequences $\boldsymbol{\tau}_n$, $\mathbf{d}_{t_n}$ and U_{i_n}.

We now state $\Delta Q_{t_n} = Q_{t_{n+1}} - Q_{t_n}$ and consider model errors and noisy measures. With (48) and (51) in (21) it results

$$\Delta Q_{t_n} = \Big((I - hK_p)\,\tilde{\boldsymbol{\eta}}_{t_n}+h\left(J_{t_n}\tilde{\mathbf{v}}_{t_n}+\dot{\boldsymbol{\eta}}_{r_{t_n}}\right)+ \tag{53}$$

$$+\,\boldsymbol{\eta}_{r_{t_n}}-\boldsymbol{\eta}_{r_{t_{n+1}}}+\boldsymbol{\varepsilon}_{\eta_{n+1}}+\delta\boldsymbol{\eta}_{t_{n+1}}\Big)^{2}-\tilde{\boldsymbol{\eta}}_{t_n}^{2}+$$

$$+\Bigg(\tilde{\mathbf{v}}_{t_n}+J_{t_n}^{-1}\dot{\boldsymbol{\eta}}_{r_{t_n}}-J_{t_n}^{-1}K_p\tilde{\boldsymbol{\eta}}_{t_n}-J_{t_{n+1}}^{-1}\dot{\boldsymbol{\eta}}_{r_{t_{n+1}}}+J_{t_{n+1}}^{-1}K_p\tilde{\boldsymbol{\eta}}_{t_{n+1}}+$$

$$+\,h\Bigg(M^{-1}\Bigg(-\sum_{i=1}^{6}\left(C_{c_i}-U_{i_n}\right).\times C_{v_i}\mathbf{v}_{t_n}-\left(D_l-U_{\gamma_n}\right)\mathbf{v}_{t_n}-$$

$$-\sum_{i=1}^{6}(D_{q_i}-U_{i+\gamma_n})\,|v_{i_{t_n}}|\mathbf{v}_{t_n}-(B_1-U_{14_n})\,\mathbf{g}_{1_{t_n}}-(B_2-U_{15_n})\,\mathbf{g}_{2_{t_n}}-$$

$$-U_{16_n}\mathbf{d}_{t_n}-J_{t_n}\tilde{\boldsymbol{\eta}}_{t_n}-K_v\tilde{\mathbf{v}}_{t_n}\Bigg)\Bigg)+\delta\mathbf{v}_{t_{n+1}}+\boldsymbol{\varepsilon}_{v_{n+1}}\Bigg)-\tilde{\mathbf{v}}_{t_n}^{2}.$$

It is worth remarking that $\boldsymbol{\tau}_n$ does not cancel all the sign-undefined terms in (53) because $\boldsymbol{\tau}$ was designed upon $\dot{Q}$ and not upon ΔQ_{t_n}.

Similarly as done in (25), we develop the squares onto (53) and make U_{i_n} to tend to the values $U^*_{i_n}$'s of (27)-(29). So, one attains

$$\begin{aligned}\Delta Q^*_{t_n} &= \overset{\frown}{\boldsymbol{\eta}}^{T}_{t_n} hK_p\left(hK_p - 2I\right)\overset{\frown}{\boldsymbol{\eta}}_{t_n} + \\ &+\overset{\frown}{\mathbf{v}}^{T}_{t_n} h\left(K^*_v M\left(hK^*_v - I\right) - MK^*_v\right)\overset{\frown}{\mathbf{v}}_{t_n} \\ &+f_{\eta,v} + f_{\delta,\varepsilon},\end{aligned} \tag{54}$$

with the two sign-undefined components, namely a similar to the previous error function in (39), a new $f_{\delta,\varepsilon}$ and a undefined-sign state-dependent new function

$$f_{\eta,v} = \left(h(J_{t_n}\overset{\frown}{\mathbf{v}}_{t_n} + \dot{\boldsymbol{\eta}}_{r_{t_n}}) + \boldsymbol{\eta}_{r_{t_n}} - \boldsymbol{\eta}_{r_{t_{n+1}}}\right)^2 + \tag{55}$$

$$+h^2\overset{\frown}{\boldsymbol{\eta}}^{T}_{t_n} J_{t_n} M^{-T} J^{T}_{t_n}\overset{\frown}{\boldsymbol{\eta}}_{t_n} + 2\left(h\left(J_{t_n}\overset{\frown}{\mathbf{v}}_{t_n} + \dot{\boldsymbol{\eta}}_{r_{t_n}}\right) + \boldsymbol{\eta}_{r_{t_n}} - \boldsymbol{\eta}_{r_{t_{n+1}}}\right)^T$$

$$\left(I - hK_p\right)\overset{\frown}{\boldsymbol{\eta}}_{t_n} - h\overset{\frown}{\boldsymbol{\eta}}^{T}_{t_n} J^{T}_{t_n} M^{-T} M\left(I - hK^*_v\right)\overset{\frown}{\mathbf{v}}_{t_n} -$$

$$-h\overset{\frown}{\mathbf{v}}^{T}_{t_n}\left(I - hK^*_v\right)^T J^{T}_{t_n}\overset{\frown}{\boldsymbol{\eta}}_{t_n}.$$

It is worth emphasized that this term is not present in the first design.

Herein, it is equally supposed that K_p and K^*_v are so chosen that satisfy conditions (42)-(43).

If the disturbances and model errors in measured states disappear, then $f_{\delta,\varepsilon} = 0$. However, this is not the case with the new term $f_{\eta,v}$ in (55) that arises only in $\Delta Q^*_{t_n}$ of the second controller design. This is very critical because it compromises the stability still when $f_{\delta,\varepsilon} = 0$.

To evidence this instability let us suppose J_{t_n} is large (which typically occurs for instance by a pitch angle $\theta \gtrapprox 40$ degrees). In consequence, still for h small, the positive-defined terms $\left(hJ_{t_n}\overset{\frown}{\mathbf{v}}_{t_n}\right)^2$ and $h^2\overset{\frown}{\boldsymbol{\eta}}^{T}_{t_n} J_{t_n} M^{-T} J^{T}_{t_n}\overset{\frown}{\boldsymbol{\eta}}_{t_n}$ in (55), may accomplish

$$\begin{aligned}&h\,\overset{\frown}{\boldsymbol{\eta}}^{T}_{t_n} J_{t_n} M^{-T} J^{T}_{t_n}\overset{\frown}{\boldsymbol{\eta}}_{t_n} + h\,\overset{\frown}{\mathbf{v}}^{T}_{t_n} J^{2}_{t_n}\overset{\frown}{\mathbf{v}}_{t_n} > \\ &> \overset{\frown}{\boldsymbol{\eta}}^{T}_{t_n} K_p\left(2I - h\right)\overset{\frown}{\boldsymbol{\eta}}_{t_n} + \overset{\frown}{\mathbf{v}}^{T}_{t_n}\left(K^*_v M\left(hK^*_v - I\right) - MK^*_v\right)\overset{\frown}{\mathbf{v}}_{t_n}\end{aligned} \tag{56}$$

for $\overset{\frown}{\boldsymbol{\eta}}_{t_n}(0), \overset{\frown}{\mathbf{v}}_{t_n}(0) \neq \mathbf{0}$ and the control system is potentially unstable.

This property let us conclude that a simple translation of an analog high-performance adaptive controller in the discrete time domain is inherently unstable.

V. Case study

In this section we present simulations of the control for a full actuated underwater vehicle described in [Jordán and Bustamante, 2009] in the context of a path-tracking problem in 6 degrees of freedom. The geometric reference path concerns a planar motion with immersions to the sea floor where the vehicle mass is changed according to Fig. 2. The programmed reference velocity vector was chosen according to a high cruise speed (both in rectilinear stretches and curves).

The goal in this Section is to illustrate the vehicle behavior in the light of the obtained results of digital adaptive controllers. Here, the two described approaches are simulated comparatively.

The most important *a-priori* information for the adaptive controller design is the ODE-structure in (1)-(2). The values of the dynamics matrices are assumed unknown for the adaptive controllers with the exception of the lower bound for the inertia matrix M. This takes the form

$$M = M_b + M_a \tag{57}$$

with the body matrix M_b and the additive matrix M_a given by

$$M_b = M_{b_n} + \delta(t - t_{A'})\, M_{b\Delta^+} - \delta(t - t_{B'})\, M_{b\Delta^-} \tag{58}$$

$$M_a = M_{a_n} + \delta(t - t_{A'})\, M_{a\Delta^+} - \delta(t - t_{B'})\, M_{a\Delta^-} \tag{59}$$

where M_{b_n} and M_{a_n} are nominal values of M_b and M_a at the start point O, and $M_{b\Delta^-}, M_{b\Delta^+}, M_{a\Delta^+}$ and $M_{a\Delta^-}$ are positive and negative variations at instants $t_{A'}$ and $t_{B'}$ on the points A' and B' of Fig. 2. Here $\delta(t - t_i)$ represents the Dirac function.

For our application M_{b_n} is experimentally determinable beforehand and the resulting value is given to the required lower bound $\underline{M}$. In the simulated scenario, $M_{b\Delta^-}$ represents the known mass of an equipment deposited on the seafloor. However $M_{b\Delta^+}$, $M_{a\Delta^+}$ and even $M_{a\Delta^-}$, are unknown for the adaptive controllers. The property of $M_a \geq 0$ is not affected by the sign of its variations $M_{a\Delta^+}$and $M_{a\Delta^-}$. For that reason, a valid lower bound is chosen as $\underline{M} = M_{b_n} - M_{b\Delta^-}$.

Taking into account the simulation setup for the weight changes (one weight picked up from the seafloor at $t_{A'}$ and the second weight deposited on the seafloor at $t_{B'}$), the lower bound for $\underline{M}$ is

$$\underline{M} = \mathrm{diag}(60, 60, 60, 5, 10, 10), \tag{60}$$

and the mass variations are

$$\begin{aligned}M_{b_n} &= diag(80, 80, 80, 4.39, 8.06, 9.17)\\ M_{a_n} &= diag(75, 126, 308, 2.3, 5.21, 5.51)\\ M_{b\Delta^+} &= \mathrm{diag}(10, 10, 10, 0.6250, 4.2250, 3.6)\\ M_{b\Delta^-} &= \mathrm{diag}(20, 20, 20, 1.25, 1.25, 0)\\ M_{a\Delta^+} &= \mathrm{diag}(6.3, 15.4, 0.115, 0.115, 0.261, 0.276)\\ M_{a\Delta^-} &= \mathrm{diag}(12.6, 30.8, 0.23, 0.23, 0.521, 0.551).\end{aligned}$$

Besides M_b and M_a we have the physical matrices of the

ROV dynamics

$$
\begin{array}{lll}
D_{q_{11}} = 130\,|u| & D_{q_{22}} = 195\,|v| & D_{q_{33}} = 286\,|w| \\
D_{q_{44}} = 5.0052\,|p| & D_{q_{55}} = 10.5485\,|q| & D_{q_{66}} = 10.1787\,|r| \\
D_{q_{42}} = 48.75\,|v| & D_{q_{51}} = 32.5\,|u| & \\
D_{q_{ij}} = 0 \text{ for the remainder terms} &&
\end{array}
$$

$$
\begin{array}{lll}
D_{l_{11}} = 6.5 & D_{l_{22}} = 9.75 & D_{l_{33}} = 14.3 \\
D_{l_{44}} = .1747 & D_{l_{55}} = .3682 & D_{l_{66}} = .3553 \\
D_{l_{42}} = 2.4375 & D_{l_{51}} = 1.5625 & \\
D_{q_{ij}} = 0 \text{ for the remainder terms} &&
\end{array}
$$

where $C_b(v)$, $C_a(v)$ and $\mathbf{g}$ were deduced from M_b and M_a (see [Fossen, 1994]).

According to (42) the controller design gain matrices were selected for a proposed sampling time of $h = 0.05$(s). So

$$
\begin{aligned}
K_p &= \frac{I}{h} = (20, 20, 20, 20, 20, 20) \\
K_v &= \frac{M}{h} = \text{diag}\,(1200, 1200, 1200, 100, 200, 200)
\end{aligned}
$$

and the adaptive gain matrices about

$$\Gamma_i = I. \tag{61}$$

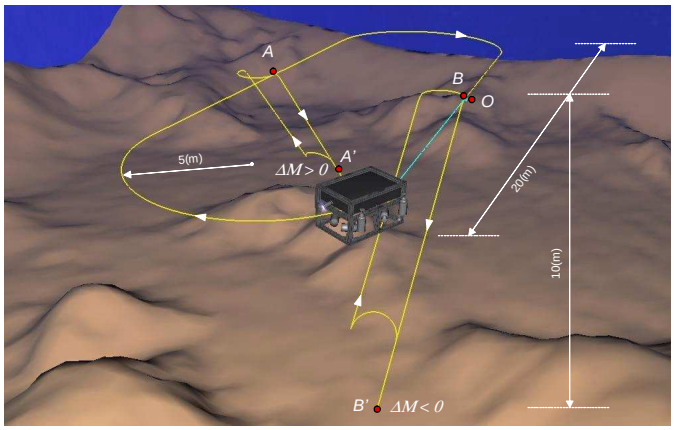

Fig. 2 - Path tracking with grab sampling (A'), and with placing of an equipment on the seafloor (B')

Figs. 3 and 4 present the control performance for the two approaches labelled as DAC (Digital Adaptive Control of the design I) and DAAC (Digitalized Analog Adaptive Control of the design II). The design matrices were tuned appropriately for the both approaches.

Comparatively, the path errors were much more larger both in position and kinematics for the digitalized approach DAAC. This had occurred in all transients. The steady-state performance show a similar disproportion between both algorithms in favour of our approach. Additionally, the DAAC turns unstable by other selection of the design matrices K_v and K_p. This is illustrated in the first period of the simulation. On the contrary, the DAC also maintains its stability for higher sampling time (h about 0.5(s)) meanwhile the DAAC turns unstable.

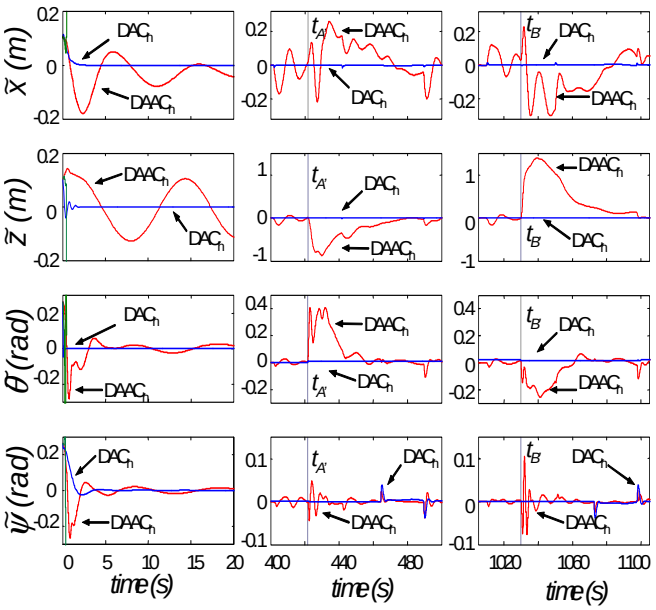

Fig. 3 - Comparative time evolution of geometric path errors during transients

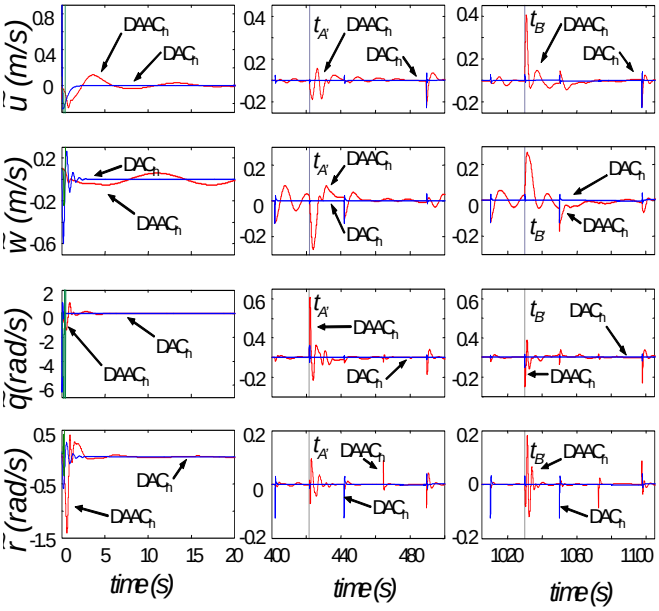

Fig. 4 - Comparative time evolution of rate path errors during transients

VI. Conclusions

In this paper two design approaches for digital adaptive controllers oriented to complex dynamics were developed. The application field for the system class is the guidance of underwater vehicles in the context of path tracking problems. The first design approach is developed entirely on the discrete time domain and employs speed-gradient techniques and first order approximation models. Conditions for accomplishing convexity of the adaptive laws and asymptotic stability are derived. The second design approach is based on the digitalization of the same but analog speed-gradient technique. In both approaches noisy measures and

model errors were considered.

A particularity of the designed digital adaptive control is the need of providing a lower bound of the inertia matrix, which is totally plausible in the system class we are contemplating through the body inertia matrix.

A substantial difference between both approaches had emerged from the stability analysis. While the design *II* with the digitalized analog adaptive controller show potentially unstable behavior when the sampling time is not "sufficiently" small to fulfill a particular inequality, the digital adaptive control system of the design *I* is always stable. The influence of noisy measures and model errors is about the same in both cases and may be attenuated by choosing a small h.

Finally, a case study emulating a sampling mission was simulated. Features indicated in the theory could be evidenced in the control behavior of both approaches.

References

Antonelli, G. (2006). An adaptive law for guidance and control of remotely operated vehicles. In 14th Mediterranean Conference on Control and Automation (MED'06), Ancona, Italy.

Fossen, T.I. (1994). *Guidance and control of ocean vehicles*, John Wiley&Sons, New York.

Fradkov, A.L., Miroshnik, I.V. and Nikiforov, V.O. (1999). *Nonlinear and adaptive control of complex systems.* Klu-Kluwer Academic Publishers, Dordrecht

Jordán M.A. and Bustamante, J.L. (2008). Guidance of underwater vehicles with cable tug perturbations under fixed and adaptive control modus. *IEEE of Oceanic Engineering*, 33 (4), 579-598.

Jordán M.A. and Bustamante, J.L. (2009). Adaptive control for guidance of underwater vehicles. *In Underwater Vehicles*, In-Tech, Vienna, Austria, A.V. Inzartev (Ed.), Chapter 14, 251-278.

Jordán, M.A., Bustamante, J.L. and Berger, C.E. (2010). Adams-Bashforth sampled-data models for perturbed underwater-vehicle dynamics. *In IEEE/OES South America Int. Symp.*, Buenos Aires, Argentina.

Kinsey, J.C., Eustice, R.M. and Whitcomb, L.L. (2006). A survey of underwater vehicle navigation: Recent advances and new challenges. *In Proceedings of the 7th IFAC Conference of Manoeuvering and Control of Marine Craft*, Lisbon, Portugal.

Krstić, M. , Kanellakopoulus, I. and Kokotović, P.V. (1995). *Nonlinear and adaptive control design.* John Wiley and Sons, New York.

Smallwood, D.A. and Whitcomb, L.L. (2003). Adaptive identification of dynamically positioned underwater robotic vehicles. *IEEE Trans. on Control Syst. Technology*, 11 (4), 505-515.